Investigation on the Effects of Fabrication Parameters on the Structure and Properties of Surface-Modified Membranes Using Response Surface Methodology

Gh. Bakeri,[1,2] A. F. Ismail,[1] D. Rana,[3] T. Matsuura,[3] M. Shariaty[4]

[1]*Faculty of Chemical Engineering, Babol Noshirvani University of Technology, Babol, Iran*
[2]*Advanced Membrane Technology Research Centre (AMTEC), Universiti Teknologi Malaysia, 81310 Skudai, Johor, Malaysia*
[3]*Industrial Membrane Research Institute, Department of Chemical and Biological Engineering, University of Ottawa, Ottawa, ON, Canada K1N 6N5*
[4]*School of Chemical Engineering, College of Engineering, University of Tehran, 11365-4563 Tehran, Iran*

Received 17 November 2010; accepted 27 April 2011
DOI 10.1002/app.34802
Published online 1 September 2011 in Wiley Online Library (wileyonlinelibrary.com).

ABSTRACT: Surface Modifying Macromolecules (SMM) were used to alter the hydrophobicity of polyetherimide (PEI) hollow fiber membranes and the effects of three fabrication parameters, which are the mass fraction of PEI and SMM in the casting dope and air gap, on the properties of fabricated membranes were investigated by application of Response Surface Methodology (RSM). The fabricated membranes were characterized in terms of mean pore size ($r_{P,m}$), permeation rate of helium gas at 1 bar transmembrane pressure difference, membrane porosity, and contact angle of water with inner and outer surfaces of membrane. The regression models obtained for mean pore size and permeation rate have good statistical parameters and are accurate. The model for $r_{P,m}$ predicts that plot of $r_{P,m}$ versus air gap has a minimum point, whereas the plots of $r_{P,m}$ versus PEI (wt %) and SMM (wt %) have maximum points. The regression model developed for membrane porosity predicts that membrane porosity decreases when air gap increases. Since water was used as bore fluid, the model developed for inner surface contact angle has low accuracy but the model developed for outer surface contact angle predicts that contact angle increases with SMM concentration in dope solution but there is a maximum point versus air gap. © 2011 Wiley Periodicals, Inc. J Appl Polym Sci 123: 2812–2827, 2012

Key words: polyetherimide hollow fiber membrane; surface modifying macromolecule; response surface methodology; hydrophobicity; contact angle

INTRODUCTION

It is well known that the morphology and the surface properties of membranes have important effects on the membrane performance in various separation processes.[1,2] For example, surface porosity and pore size, surface roughness, surface charge, and hydrophobicity/hydrophilicity of membranes are important parameters to govern membrane performance in the processes such as ultrafiltration, nanofiltration, membrane distillation, and membrane contactor. It has been reported that membrane surface hydrophobicity has a strong effect on the fouling of ultrafiltration membranes in separation of humic acids from water.[3] As well, hydrophobicity should be high enough for the membranes used in membrane contactor and membrane distillation processes as penetration of liquid into membrane pores reduces the performance drastically.

Correspondence to: A. F. Ismail (afauzi@utm.my).

Journal of Applied Polymer Science, Vol. 123, 2812–2827 (2012)

Different approaches have been proposed for membrane surface modification to change the hydrophobicity/hydrophilicity of the membrane surface. They include photochemical grafting,[4–8] ion beam irradiation,[9] redox-initiated graft polymerization,[10,11] low temperature plasma treatment,[12,13] and UV-assisted grafting.[1] These methods can be further classified in three main categories: 1—physical modification, 2—chemical modification, and 3—bulk modification. However, all of them have some disadvantages such as:

1. The process is a two-stage process; i.e., an extra process is necessary for membrane surface modification.
2. The processes can change not only the surface properties but also the bulk properties of the membrane.
3. Most of the above processes are difficult to be used in a commercial scale.

One interesting method to change the hydrophobicity of membrane is blending of Surface Modifying Macromolecule (SMM) to the casting dope. Hydrophobic

SMMs are macromolecules with an amphipathic structure. Their main chain consists of a polyurea or polyurethane polymer (hydrophilic part), which is end capped with two low polarity fluorine-based polymer (oligomer) chains (hydrophobic part). Since SMM has a lower surface energy, it tends to migrate, during the membrane fabrication process, to the membrane–air interface to minimize the system's interfacial energy, making nanoscale agglomerates at the surface of the membrane.[14] As a consequence, the surface properties of the membrane change. In particular, the fluorine-based chains at both ends of SMM orient themselves vertical to the membrane–air interface.[15] This makes the surface more hydrophobic and also gives some other features, such as surface lubrication and chemical resistance due to the carbon–fluorine chemical bond, to the membrane surface.[3] It was also reported that the SMM modified PES membrane has higher mechanical strength compared with the unmodified membrane.[16] Furthermore, as only a small amount of SMM is blended to the host polymer, the bulk properties of membrane do not change.

The mechanism and kinetics of SMM surface migration were discussed elsewhere.[17,18] It was reported that blending of SMM to polyethersulfone flat sheet membrane increased the contact angle from 76° to 116°, a value close to the contact angle of inherently hydrophobic polymers such as polytetrafluorethylene (PTFE).[2] The degree of SMM surface migration depends on the molecular structure and the molecular weight of SMM and the length of the fluorohydrocarbon end group. The SMM surface migration is also affected by the membrane fabrication conditions such as; the temperature of casting dope, concentrations of host polymer, SMM and other additives in the casting dope, solvent used for preparation of the casting dope, and time between film casting and immersion into the coagulation bath. SMM migration takes place only before the polymer solidifies by the solvent–nonsolvent exchange.

Many researches have been done on the membrane surface modification using SMM and the effect of SMM blending on membrane performance. Most of these investigations were devoted to flat sheet membranes[19–23] with few exceptions of dealing with hollow fiber membranes.[15,24] It should be noted that there are some differences between the flat sheet and hollow fiber membranes. When the flat sheet membrane is fabricated, solvent/nonsolvent exchange initiates from one side of the membrane cross section. On the other hand, solvent/nonsolvent exchange proceeds from both sides of the cross section of the hollow fiber membrane. Furthermore, unlike the flat sheet membrane, in hollow fiber spinning process, the polymer solution is subjected to various kinds of stresses as it is extruded through the channel of a spinneret, by which macromolecules undergo orientation and packing, resulting in the change in the morphology and the surface properties of the membrane.[25] As soon as the nascent fiber exits the spinneret and begins to travel along the air gap, its inner surface undergoes phase inversion. In contrast, the outer surface experiences coalescence and orientation of polymer aggregates, stress relaxation, and also elongation due to gravity before the fiber enters the coagulation bath. Also, the effect of air humidity and vapor induced phase separation (VIPS) process on the properties of membrane should be considered.[26] Furthermore, since SMM is a powerful nonsolvent for the polymer solution, the addition of SMM makes the solution less stable thermodynamically (changes the cloud point curve of the polymer solution).[14,18,19,27] Even though the amount of SMM involved is small, the polymer content in the casting dope nevertheless increases, which inevitably increases the solution viscosity[28] and affects the kinetics of SMM migration and phase inversion. These dual effects of polymeric additives, such as PVP, on thermodynamic stability and viscosity of polymer solution, which influences the phase inversion process, has been reported elsewhere.[29,30]

The most significant difference between the flat sheet and hollow fiber membrane fabrication is, however, the time between the film casting (or polymer dope extrusion from spinneret in case of hollow fiber) and the immersion into the coagulation bath. During this period, the solvent may evaporate from the membrane surface, if the solvent is sufficiently volatile, and/or the macromolecules at the membrane surface may undergo relaxation. While this time may be stretched to infinity, at least theoretically, in the flat sheet membrane fabrication, the time is limited, in reality, to few seconds, for the hollow fiber spinning, depending on the air gap length. This means the time allowed for the SMM surface migration is very limited when hollow fibers are spun.

Application of a statistical approach seems most logical to investigate the effects of the variables involved in hollow fiber spinning, particularly when SMM is blended into the spinning dope, since the spinning parameters must be interrelated to each other in such a complicated system. However, to the authors' knowledge, the Response Surface Methodology (RSM) has never been applied so far to investigate the hollow fiber spinning process in the presence of SMM in the casting dope. Hence, it is the objective of this research to investigate the effects of blending hydrophobic SMM into the spinning dope on the properties of the polyetherimide hollow fiber membrane in terms of mean pore size and gas permeation rate, membrane porosity, and hydrophobicity of the membrane. The above characterization parameters

TABLE I
Investigated Factors and Their Levels in the Experimental Design

Factor	Levels				
	−1.682	−1	0	+1	+1.682
PEI (wt %) in casting dope	14 (13.9955)[a]	14.2	14.5	14.8	15 (15.0045)
SMM (wt %) in casting dope	0.002 (0.00206)	0.51	1.255	2	2.508 (2.50794)
Air gap (cm)	0.89 (0.887)	21	50.5	80	100.1 (100.113)

[a] The values in the parentheses represent the designed values for factors which were not applied in the experimental runs.

were chosen since they are known to govern the membrane performance when the membrane is used for the membrane contactor process. The membrane contactor test results of these membranes will be presented in the upcoming publication.

As well, the following three membrane fabrication parameters were chosen, since they seem to govern the membrane characteristics and performance most strongly.

1. PEI concentration in the casting dope;
2. SMM concentration in the casting dope; and
3. Air gap.

RESPONSE SURFACE METHODOLOGY (RSM)

In Response Surface Methodology (RSM), a model with the form of eq. (1) is fitted to experimental data and, by optimization methods, the best coefficients for the model are calculated.

$$Y = a_0 + \sum_{i=1}^{f} a_i x_i + \sum_{i=1}^{f} a_{ii} x_i^2 + \sum_{i<j}^{f} a_{ij} x_i x_j + \zeta \qquad (1)$$

where f is the number of factors, $\{x_i\}$ are linear terms, $\{x_i^2\}$ are quadratic terms, and $\{x_i x_j\}$ are interaction terms, Y is response (experimental data), and ζ is the difference between experimental data and the results predicted by model. $\{a_i\}$, $\{a_{ii}\}$, and $\{a_{ij}\}$ are the coefficients of the model. The adequacy of the model and significance of the coefficients should be analyzed by statistical methods. The model can be validated using, Fisher F-test,[31] P-value of the model, R^2 and R^2-adjusted. The values of test statistics (F-value = variance between samples/variance within samples) and probability (P-value) were then calculated for each of the seven combinations. A significance level of 95% was chosen, thus combination with a P-value less than 0.05 was considered to be significant.

Central Composite Design (CCD) for response surface modeling was used for design of experiments to investigate the effect of SMM on the properties of the polyetherimide hollow fiber membrane. The investigated factors and their levels are shown in Table I where the α value (axial spacing) is 1.682.

Mean pore size of the membranes, helium gas permeance, membrane porosity, and contact angles of water at the inner and outer surfaces of membrane were chosen as the responses. Minitab software, release 15 was used to analyze the experimental results. The guidelines presented by this software were used for elimination of terms in the model. Based on these guidelines, the terms with a P-value greater than 0.05 should be eliminated while R^2-adjusted increases. In some cases, after elimination of a term with a P-value greater than 0.05, R^2-adjusted decreases which means that although the term has insignificant influence on the model, the effect on the response is significant enough to be included in the model.

EXPERIMENTAL

Materials

Polyetherimide (PEI, Ultem®), used as the base polymer, was purchased from General Electric Company. *N*-methyl-2-pyrrolidone (NMP) (CAS Number: 872-50-4) with purity of 99.5 wt % and ethanol (CAS number: 64-17-5) with purity of 96 wt % were purchased from Merck and used without any purification.

The details of SMM synthesis have been given elsewhere.[32] The SMM utilized herein, was synthesized from methylene bis(*p*-phenyl isocyanate) (diphenylmethane diisocyanate; MDI), α,ω-aminopropyl poly (dimethyl siloxane) (PDMS), and Zonyl BA-L™ low fraction (2-(perfluoroalkyl)ethanol; BAL). The SMM was further characterized by elemental analysis and gel permeation chromatography (GPC, Waters Associates GPC chromatograph equipped with Waters 410 refractive index detector). The results, atomic percentage of fluorine and silicone obtained from the elemental analysis and number averaged molecular weight, M_n, and polydispersity, PDI, both obtained from GPC, are presented in Table II.

The structure of SMM, determined from the above characterization results, is shown in Figure 1, where p is the number of the CF_2 repeating unit and equal to 7.58, n is the number of the PDMS repeating unit and equal to 9.81, and m is the number of the urea repeating unit and equal to 13.10.

TABLE II
SMM Characterization Results

F (wt %)	Si (wt %)	M_n (10^4 g/mol)	PDI
16.21	12.82	1.62	1.82

Polydispersity = M_w/M_n.

Dope preparation

PEI was dried at 70°C overnight. PEI solution (20 wt %) was prepared by dissolving a predetermined amount of PEI in NMP at 60–70°C under gentle stirring. SMM solution (6 wt %) was prepared by dissolving SMM in NMP at room temperature with gentle stirring.

PEI and SMM solutions were combined to prepare the spinning dope of the desired compositions. Then, the solution was left standing for degassing.

Preparation of hollow fibers

The hollow fiber membranes were fabricated by the dry-wet spinning process. The fabrication process was described elsewhere in detail.[33] A tube-in-orifice spinneret was used for dope extrusion. A pressure of N_2 gas was used to deliver the dope solution to a gear pump by which the dope solution was brought to the annulus of the spinneret at a constant flow rate. Distilled water was used as the bore fluid which was delivered to the inner tube of the spinneret by a peristaltic pump at a constant flow rate.

After leaving the spinneret, the nascent hollow fiber passed through the air gap before entering the coagulant (water) bath to complete the phase inversion process. The hollow fibers were then collected by a take up drum and kept immersed in water for several days before solvent exchange was conducted by immersing the hollow fibers in water/ethanol mixtures of progressively higher ethanol concentrations.

1. 1 h in 33 wt % ethanol solution in water.
2. 1 h in 66 wt % ethanol solution in water.
3. 2 h in pure ethanol.

The hollow fibers were further dried naturally by hanging vertically for 1 to 2 days at ambient temperature. The spinning conditions were listed in Table III.

Hollow fiber module preparation and gas permeation test

Gas permeation test is a common method for determination of mean pore size ($r_{P,m}$) and effective surface porosity, which is defined as the ratio of surface porosity (ξ) to effective pore length at the skin layer (L_P).[34–36] Two to three hollow fibers were glued with epoxy resin at one end and the other end was potted to stainless steel tubing with a diameter of 1.4 cm. The latter end was cut using a sharp knife after the epoxy resin was hardened to open the hollow fibers.[37] The hollow fiber module so prepared and the gas permeation test system are shown schematically in Figure 2.

Helium gas was supplied to the shell side and helium permeation rate was measured at transmembrane pressure differences from 1 to 4 bar by a soap bubble flow meter connected to the lumen side of the hollow fiber bundle. The effective area of the hollow fiber bundle in the module was 6–15 cm^2.

From a straight line relationship between gas permeance, in terms of $\frac{\text{mol}}{\text{m}^2\text{Pa s}}$ and mean pressure (Pa), defined as $\frac{p_u+p_d}{2}$ where p_u and p_d are upstream and downstream pressure, respectively, slope (B) and intercept (A) are obtained. The mean pore size ($r_{P,m}$) and the effective surface porosity ($\frac{\xi}{L_P}$) are calculated from (B) and (A) using eqs. (2) and (3).

$$r_{P,m} = \frac{16}{3}\frac{B}{A}\left(\frac{8\text{RT}}{\pi M}\right)^{0.5}\mu \tag{2}$$

$$\frac{\xi}{L_P} = \frac{8\mu\text{RT}B}{r_{P,m}^2} \tag{3}$$

where R is the universal gas constant (8.314 J mol^{-1} K^{-1}), T is absolute temperature (K), M is molecular weight of helium (Kg mol^{-1}), $r_{P,m}$ is mean pore radius (m), μ is viscosity of gas (Pa s), ξ is surface porosity ($\frac{A_P}{A_T}$ where A_P is area of pores and A_T is total area of membrane), and L_P is effective pore length (m).

The permeation rate of helium gas at 1 bar transmembrane pressure difference, presented as $\frac{10^6\text{cm}^3(\text{STP})}{\text{cm}^2.\text{sec.cmHg}}$, was used as a criterion for gas

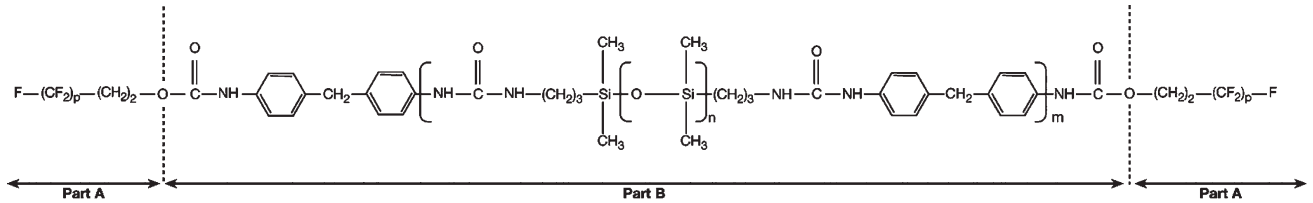

Figure 1 Structure of Surface Modifying Macromolecule (SMM).

TABLE III
Hollow Fiber Spinning Conditions

Polymer concentration (wt %)	Based on designed experiments which are shown in Table IV
SMM concentration (wt %)	Based on designed experiments which are shown in Table IV
Air gap (cm)	Based on designed experiments which are shown in Table IV
Bore fluid	Distilled water
External coagulant	Tap water
Spinneret o.d./i.d. (mm)	1.3/0.55
Bore fluid temperature (°C)	Room temperature
External coagulant temperature (°C)	Room temperature

permeability of the membranes and named as Gas Permeation Unit (GPU).

Contact angle measurement

The contact angle of the inner and outer surface of the membranes was measured by the sessile drop technique using contact angle goniometer (model G1, Krüss GmbH, Hamburg, Germany) and water as the liquid. To measure the contact angle of the inner surface, the wall of hollow fiber was cut with a small knife and then the fiber was opened to make a flat surface. For the outer surface, no preparation was done. At least 10 points were used for the contact angle measurement and the average value was calculated.

Membrane porosity

The bulk membrane porosity was measured by the method presented by Chabot et al.[38] The membrane porosity was calculated by eq. (4).

$$\varepsilon = \frac{\frac{1}{\rho_m} - \frac{1}{\rho_P}}{\frac{1}{\rho_m}} \tag{4}$$

where ε is membrane porosity, ρ_P is polymer density (1.27 g cm^{-3} for PEI), and ρ_m is membrane density which is calculated by eq. (5).

$$\rho_m = \frac{G}{(\frac{G}{\rho_P} + \frac{1-G}{\rho_{water}})(1-E)} \tag{5}$$

where ρ_{water} is density of water, G is mass fraction of polymer in the membrane and E is overall shrinkage of the membrane during drying. G and E are calculated by eqs. (6) and (7), respectively.

$$G = \frac{\text{dry membrane weight}}{\text{wet membrane weight}} \tag{6}$$

$$E = 1 - (1 - S_l)^3 \tag{7}$$

where S_l, the longitudinal shrinkage of hollow fiber, was obtained by eq. (8).

$$S_l = \frac{\text{wet membrane length} - \text{dry membrane length}}{\text{wet membrane length}} \tag{8}$$

Several wet spun hollow fibers were kept in water for several days to remove the residual solvent. Then, the water in the lumen side of hollow fiber was blown off and the membrane was weighed to obtain the wet weight. The length of the wet membranes was also measured. The hollow fibers then were dried in an oven at 40–45°C overnight and the weight and the length of the dried fibers were measured.

Scanning electron microscopy (SEM) and energy dispersive X-ray (EDX)

The hollow fiber was fractured in liquid nitrogen to observe its cross section. To observe the inner surface, the hollow fiber was cut to make a flat surface. The outer surface was observed without any preparation. The samples were then coated by sputtering Pt. The SEM and EDX observation was done by the instrument ZEISS, SUPRA 35VP.

RESULTS AND DISCUSSION

The designed experiments in their coded and uncoded forms are shown in Table IV. The response values corresponding to each run are also shown in Table IV.

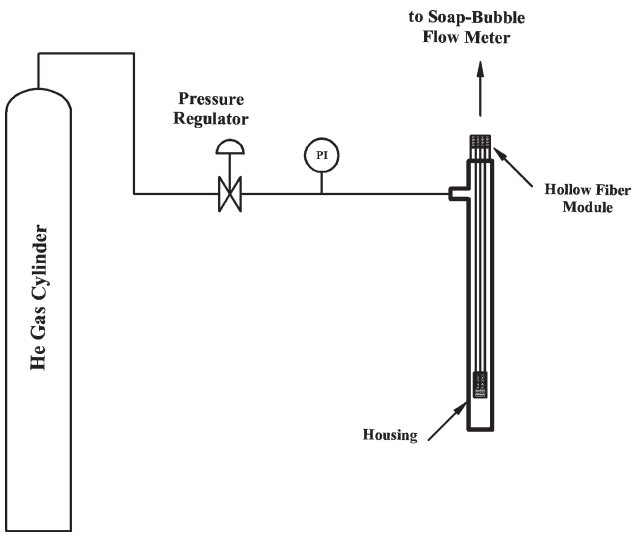

Figure 2 Schematic of gas permeation test system.

TABLE IV
The Designed Experiments and Output Responses for SMM-Modified PEI Membranes

		Fabrication parameters						Responses				
Membrane number	Run type[a]	PEI in dope solution (x_1) wt %	Level[c]	SMM in dope solution (x_2) wt %	Level[c]	Air gap (x_3) cm	Level[c]	$r_{P,m}$ nm	GPU Helium @ 1 bar $\frac{10^6 cm^3(STP)}{cm^2.sec.cmHg}$	Membrane porosity %	CA[b], inner surface	CA[b], outer surface
M1	A	15.0	$+\alpha$	1.255	0	50.5	0	151.8	2766	0.786	83.1	92.8
M2	A	14.0	$-\alpha$	1.255	0	50.5	0	104.4	1301	0.805	81.5	95.9
M3	A	14.5	0	2.508	$+\alpha$	50.5	0	72.7	1781	0.782	83.4	95.3
M4	A	14.5	0	0.002	$-\alpha$	50.5	0	139.1	6898	0.798	86.6	93.8
M5	A	14.5	0	1.255	0	100.1	$+\alpha$	537.6	21000	0.762	86.5	85.8
M6	A	14.5	0	1.255	0	0.89	$-\alpha$	281.4	12617	0.812	84.7	78.1
M7	O	14.8	+1	2.0	+1	80.0	+1	218.2	4035	0.750	76.8	104.3
M8	O	14.8	+1	2.0	+1	21.0	−1	69.6	1344	0.774	88.8	95.1
M9	O	14.8	+1	0.51	−1	80.0	+1	180.2	3004	0.768	80.7	92.7
M10	O	14.8	+1	0.51	−1	21.0	−1	101.2	203	0.772	72.3	93.8
M11	O	14.2	−1	2.0	+1	80.0	+1	281.4	6395	0.765	87.5	90.6
M12	O	14.2	−1	2.0	+1	21.0	−1	34.8	2657	0.776	83.6	95.6
M13	O	14.2	−1	0.51	−1	80.0	+1	281.4	5088	0.797	86.9	89.1
M14	O	14.2	−1	0.51	−1	21.0	−1	107.5	3671	0.809	83.5	82.7
M15	C	14.5	0	1.255	0	50.5	0	123.3	3070	0.789	92.1	93.1
M16	C	14.5	0	1.255	0	50.5	0	104.4	3100	0.782	89.1	93.3
M17	C	14.5	0	1.255	0	50.5	0	161.3	2389	0.790	82.6	92.1
M18	C	14.5	0	1.255	0	50.5	0	186.6	2341	0.780	86.3	93.2
M19	C	14.5	0	1.255	0	50.5	0	94.9	1898	0.759	82.0	95.1
M20	C	14.5	0	1.255	0	50.5	0	132.8	3541	0.783	87.4	92.1

[a] C, center point; O, orthogonal design or cube point; A, star or axial point.
[b] Contact angle.
[c] −1, low value; 0, center value; +1, high value; $\pm\alpha$, star or axial point value.

To compare the properties of the hollow fiber membranes with and without SMM, the hollow fibers were spun under the same fabrication parameters as shown in Table IV but without SMM. The fabrication parameters and the responses for such hollow fibers are summarized in Table V.

ANOVA for mean pore size ($r_{P,m}$)

The response surface methodology in Minitab software, release 15 was used to find the best model for $r_{P,m}$. The estimated coefficients for the model in terms of coded factors and the *t*-value and *P*-value for each coefficient are shown in Table VI.

The significant terms in the model for $r_{P,m}$ can be ranked as follows:

$$x_3^2 > x_3 > x_2^2 > x_1x_3 > x_1^2 > x_2x_3 > x_2 > x_1$$

The analysis of variance (ANOVA) is a useful tool to qualify the regression equation and the ANOVA at 95% confidence limit for the model developed for $r_{P,m}$ is presented in Table VII.

TABLE V
The Characterization Test Results for PEI Membranes without SMM

	Fabrication parameters		Responses		
Membrane number	PEI in dope solution wt %	Air gap cm	$r_{P,m}$ nm	GPU Helium @ 1 bar $\frac{10^6 cm^3(STP)}{cm^2.sec.cmHg}$	Membrane porosity %
M21	14.0	50.5	63.2	2576	0.817
M22	14.2	21.0	69.6	708	0.779
M23	14.2	80.0	420.6	7509	0.832
M24	14.5	0.89	75.9	1552	0.803
M25	14.5	50.5	66.4	2157	0.815
M26	14.5	100.1	139.1	4242	0.806
M27	14.8	21.0	47.4	371	0.809
M28	14.8	80.0	281.4	5403	0.797
M29	15.0	50.5	53.8	2641	0.829

TABLE VI
Estimated Regression Coefficients (Coded Factors), Response: $r_{P,m}$

Term	Coefficient	S.E. coefficient	t	P
Constant	135.806	18.27	7.434	0.000
x_1: PEI (wt %)	−6.919	20.38	−0.339	0.741
x_2: SMM (wt %)	−21.933	20.38	−1.076	0.305
x_3: Air gap (cm)	132.863	20.38	6.518	0.000
x_1^2: PEI (wt %) × PEI (wt %)	−41.669	33.37	−1.249	0.238
x_2^2: SMM (wt %) × SMM (wt %)	−63.805	33.37	−1.912	0.082
x_3^2: Air gap (cm) × Air gap (cm)	239.760	33.37	7.185	0.000
$x_1\ x_3$: PEI (wt %) × Air gap (cm)	−68.198	44.79	−1.523	0.156
$x_2\ x_3$: SMM (wt %) × Air gap (cm)	50.310	44.79	1.123	0.285

The adequacy of the model was analyzed. Referring to Table VII, the F-value for the model is 13.62, which is greater than the tabulated F-value at 95% confidence limit, $F_{0.05}(f_1,f_2) = F_{0.05}(8,11) = 2.9480$. The F-value for the lack-of-fit is 2.21, which is smaller than the tabulated F-value at 95% confidence limit, $F_{0.05}(f_3,f_4) = F_{0.05}(6,5) = 4.9503$. Also, the P-value for the model is smaller than 0.05 and the P-value for the lack-of-fit is greater than 0.05. R^2 for the model is 90.83%, which means that only 9.17% of variations in the experimental data cannot be explained by the model. Furthermore, R^2-adjusted is 84.16%, which is a sufficiently high value for R^2-adjusted.[39] Therefore, the model developed for $r_{P,m}$ is considered to be adequate.

The mean pore sizes predicted by the model are compared with the experimental results in Figure 3, which shows that the predicted values fit well the experimental results.

Referring to Tables IV and V, it is interesting to note that the mean pore sizes of the SMM modified membranes are generally higher than those without SMM, which is opposite to the results obtained elsewhere for the SMM-modified PES hollow fiber membranes.[24]

Effect of membrane fabrication parameters on mean pore size ($r_{P,m}$)

The surface plots of the mean pore size versus two fabrication parameters are shown in Figure 4(a–c) while the third fabrication parameter is held constant at its central level.

As shown in Figure 4(a) for a given PEI concentration, $r_{P,m}$ has a maximum as the SMM concentration is changed. This seems due to the superimposition of the two opposing effects of SMM addition. One is its strong nonsolvent power for PEI, which enhances formation of defects due to instantaneous phase separation and the other is increase in the overall polymer concentration and the solution viscosity, which hinders the instantaneous phase separation.

In Figure 4(b,c), $r_{P,m}$ shows a minimum for a given set of PEI and SMM concentration as the air gap is changed. According to a review written on the effect of the air gap on the hollow fiber morphology,[40] the presence of the minimum depends on the nature of the polymer. Wang et al.[41] reported a trend similar to our observation in terms of the selectivity of polyetherimide gas separation membranes. It was also reported that the mean pore size showed a minimum for SMM-modified PES hollow fibers as the air gap was increased, although the effect was not strong.[24] The results were ascribed to (1) absorption of water vapor from the environment and (2) coalescence of polymer aggregates at the outer surface of the hollow fiber, which occurred while the nascent hollow fiber was travelling through the air gap.

Looking into the data for the hollow fibers M24, M25, and M26 in Table V, a minimum in $r_{P,m}$ is also found for a given PEI concentration of 14.5 wt %.

TABLE VII
Analysis of Variance (ANOVA) Table for Model; Response: Mean Pore Size ($r_{P,m}$) of SMM-Modified Membranes

Source	DF[a]	Seq SS[b]	Adj SS	Adj MS[c]	F	F-tabulated	P
Regression	8	218,603	218,603	27,325	13.62	2.9480	0.000
Residual error	11	22,069	22,069	2006			
Lack-of-fit	6	16,036	16,036	2673	2.21	4.9503	0.200
Pure error	5	6033	6033	1207			
Total	19	240,672					

$R^2 = 90.83\%$; $R^2_{\text{adjusted}} = 84.16\%$.
[a] DF, degree of freedom.
[b] SS, sum of squares.
[c] MS, mean square.

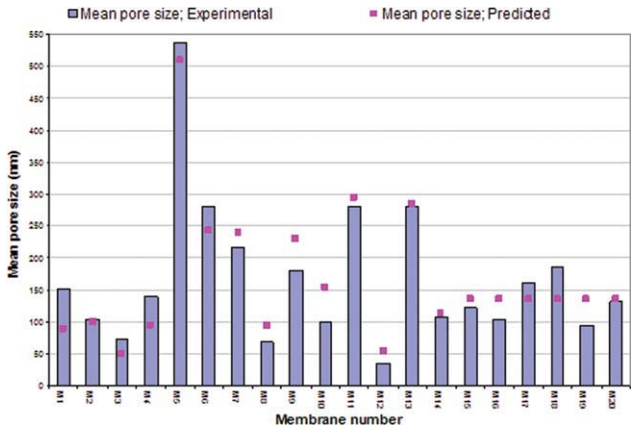

Figure 3 Comparison of experimental and predicted values by the model for mean pore size for membranes with SMM. [Color figure can be viewed in the online issue, which is available at wileyonlinelibrary.com.]

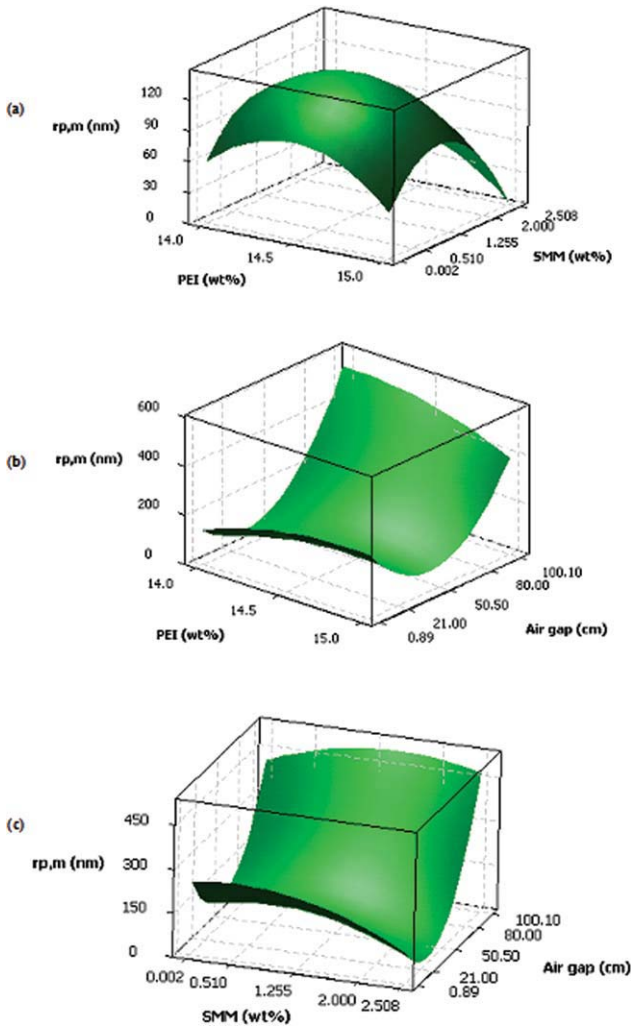

Figure 4 The surface plots for $r_{P,m}$, (a) PEI (wt %) and SMM (wt %), air gap value: 50.5 cm; (b) PEI (wt %) and air gap (cm), SMM (wt %) value: 1.255; and (c) SMM (wt %) and air gap (cm), PEI (wt %) value: 14.5. [Color figure can be viewed in the online issue, which is available at wileyonlinelibrary.com.]

TABLE VIII
Estimated Regression Coefficients (Coded Factors), Response: GPU Helium @ 1 bar

Term	Coefficient	S.E. coefficient	t	P
Constant	2526.4	913.7	2.765	0.014
x_1: PEI (wt %)	−832.6	1201.0	−0.693	0.499
x_3: Air gap (cm)	3046.6	1201.0	2.537	0.023
x_1^2: PEI (wt %) × PEI (wt %)	−3393.6	1956.6	−1.734	0.103
x_3^2: Air gap (cm) × Air gap (cm)	11380.7	1956.5	5.817	0.000

This means that a similar trend is observed with and without SMM addition to the casting dope.

ANOVA for GPU helium @ 1 bar

The response surface methodology in Minitab software, release 15 was used to find the best model for helium permeance. The estimated coefficients for the model in terms of coded factors and the P-value and t-value for each coefficient are shown in Table VIII.

The significant terms in the model for helium permeance can be ranked as follows:

$$x_3^2 > x_3 > x_1^2 > x_1$$

x_2 does not appear in this table since it has practically no effect on helium permeance. The Analysis of Variance was used to check the validity of the model and the ANOVA for the model at 95% confidence limit is shown in Table IX.

Referring to Table IX, the F-value for the model is 11.48, which is greater than the tabulated F-value at 95% confidence limit, $F_{0.05}(f_1,f_2) = F_{0.05}(4,15) = 3.0556$. The F-value for the lack-of-fit, which is 10.66, is larger than the tabulated F-value for the lack-of-fit at 95% confidence limit, $F_{0.05}(f_3,f_4) = F_{0.05}(4,11) = 3.3567$. In other words, the model has some lack-of-fit. It is also shown in the P-value for the lack-of-fit which is smaller than 0.05. The P-value for the regression is smaller than 0.05 and satisfies the criterion in this regard. R^2 for the model is 75.37%, which means that 75.37% of variations in the experimental data can be explained by the model, and R^2-adjusted is 68.80%. Both R^2 values seem reasonable. Therefore, the model developed for helium permeance can be accepted.

The comparison between the experimental and the predicted values for helium permeance is shown in Figure 5, which shows some discrepancies between these two sets of data.

Referring to Tables IV and V, the permeation rate of SMM-modified PEI membranes is generally higher than those without SMM, which can be

TABLE IX
Analysis of Variance (ANOVA) Table for Model; Response: GPU Helium @ 1 bar of SMM-Modified Membranes

Source	DF[a]	Seq SS[b]	Adj SS	Adj MS[c]	*F*	*F*-tabulated	*P*
Regression	4	3.20E+08	3.20E+08	7.99E+07	11.48	3.0556	0.000
Residual error	15	1.04E+08	1.04E+08	6.96E+06			
Lack-of-fit	4	8.30E+07	8.30E+07	2.08E+07	10.66	3.3567	0.001
Pure error	11	2.14E+07	2.14E+07	1.95E+06			
Total	19	4.24E+08					

$R^2 = 75.37\%$; $R^2_{adjusted} = 68.80\%$.
[a] DF, degree of freedom.
[b] SS, sum of squares.
[c] MS, mean square.

related to the bigger pore sizes of the SMM-modified membranes.

Effect of membrane fabrication parameters on GPU helium @ 1 bar

The surface plot of helium permeance versus PEI (wt %) and air gap is shown in Figure 6.

As depicted in Figure 6, helium permeance shows a minimum for a given PEI concentration. This trend can be related to that of $r_{P,m}$, which shows a minimum for a given PEI concentration as the air gap is increased.

ANOVA for membrane porosity

The response surface methodology in Minitab software, release 15 was used to find the best model for the membrane porosity. The estimated coefficients for the model in terms of the coded factors and the *P*-value and *t*-value for each coefficient are shown in Table X.

The terms in the model can be ranked as follows based on their significance on the response:

$$x_3 > x_1 > x_2 > x_1x_2$$

The ANOVA at 95% confidence limit of the model developed for membrane porosity is shown in Table XI and is used for model validation.

The *F*-value for the model is 6.63 which is greater than the tabulated *F*-value at 95% confidence limit, $F_{0.05}(f_1,f_2) = F_{0.05}(4,15) = 3.0556$. The *F*-value for the lack-of-fit is 1.04, which is smaller than tabulated *F*-value, $F_{0.05}(f_3,f_4) = F_{0.05}(10,5) = 4.7351$. Also, *P*-value for the model is 0.03, which is smaller than 0.05 and the *P*-value for the lack-of-fit is 0.514, which is greater than 0.05. Therefore, the model satisfies the criteria for *F*-value and *P*-value. In addition, R^2 and R^2-adjusted for the model are 63.88% and 54.25%, respectively.

The experimental and predicted values for membrane porosity are compared in Figure 7, which shows reasonable agreement between the experimental and predicted values.

Comparing the data in Tables IV and V, the membranes with SMM have generally lower membrane porosities than those without SMM.

Effect of membrane fabrication parameters on membrane porosity

The surface plots of membrane porosity versus two fabrication parameters, whereas the third parameter

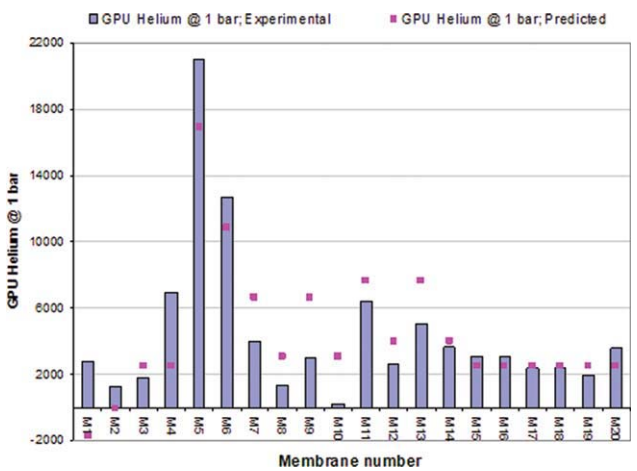

Figure 5 Comparison of experimental results and predicted values by model for GPU Helium @ 1 bar for membranes with SMM. [Color figure can be viewed in the online issue, which is available at wileyonlinelibrary.com.]

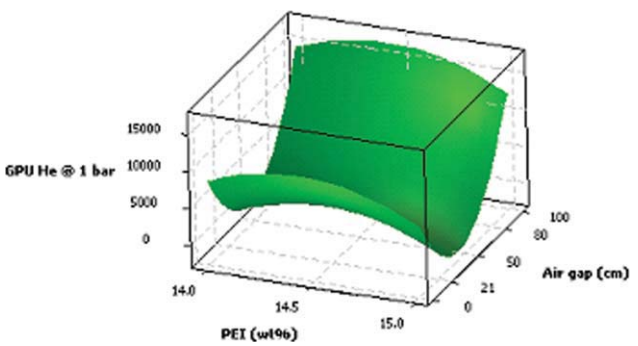

Figure 6 The surface plot of GPU Helium @ 1 bar versus PEI (wt %) and air gap (cm); SMM (wt %) value: 1.255. [Color figure can be viewed in the online issue, which is available at wileyonlinelibrary.com.]

TABLE X
Estimated Regression Coefficients (Coded Factors), Response: Membrane Porosity

Term	Coefficient	S.E. coefficient	t	P
Constant	0.78195	0.002552	306.367	0.000
x_1: PEI (wt %)	−0.01416	0.005195	−2.725	0.016
x_2: SMM (wt %)	−0.01329	0.005195	−2.558	0.022
x_3: Air gap (cm)	−0.01664	0.005194	−3.203	0.006
x_1x_2: PEI (wt %) × SMM (wt %)	0.01732	0.011414	1.518	0.150

is held constant at its central value, are shown in Figure 8(a–c).

Figure 8(a) shows that the porosity tends to decrease with the SMM concentration when the PEI concentration is as low as 14 wt %, whereas the opposite is the case when the PEI concentration is as high as 15 wt %. These two opposing trends can be explained by the following two different effects of SMM addition; one, the increase in the total (including both PEI and SMM) polymer concentration and, the other, enhancement of instantaneous phase inversion and formation of defective pores due to the hydrophobic nature of SMM. The first effect decreases the porosity, whereas the second increases the porosity. Most likely, the first effect of SMM addition is dominant when the PEI concentration is low while the second effect becomes dominant when the PEI concentration is high.

Both Figure 8(b,c) show the decrease in membrane porosity as the air gap increases.

The reason for this trend is the same as that given for the decrease of the pore size with an increase in air gap. In Figure 9, the cross-sectional SEM images for membranes No. M6, No. M16, and No. M5 are shown. The dope compositions for these three membranes are the same but the air gaps are 0.89 cm, 50.5 cm, and 100.1 cm, respectively. The images show that the length and the number of macrovoids, originating from the outer surface of membrane, decrease as the air gap increases, which in turn results in the reduction of membrane porosity.

ANOVA for inner surface contact angle

The response surface method in Minitab software, release 15 was used to fit the best model on experimental results for inner surface contact angle. The estimated coefficients of the best model with their t-values and P-values are presented in Table XII.

Using student's t-test, the coefficients can be ranked as follows based on their significance in the model:

$$x_2x_3 > x_1^2 > x_1 > x_2 > x_3$$

The ANOVA at 95% confidence limit for the model, developed for inner surface contact angle, is presented in Table XIII.

The F-value for the model is 1.48, which is not greater than the tabulated F-value at 95% confidence limit, $F_{0.05}(f_1,f_2) = F_{0.05}(5,14) = 2.9582$. The F-value for the lack-of-fit, which is 1.29, is smaller than the tabulated F-value, $F_{0.05}(f_3,f_4) = F_{0.05}(9,5) = 4.7725$. In addition, the P-value of the model is 0.258, which is greater than 0.05, but the P-value for the lack-of-fit is 0.409, which is higher than 0.05. Therefore, the model satisfies the criteria for the lack-of-fit, which means that the model has goodness-of-fit but it can not pass the criteria for regression. This further means that the model can not explain a significant amount of variations in the experimental results. In addition, considering the P-value, the model can not show the actual relations between the response and the factors. Furthermore, R^2 and R^2-adjusted for the model are 34.58% and 11.22%, respectively. These values are very low for the regression. Therefore, the developed model is not suitable for the inner surface contact angle.

The comparison between the experimental and the predicted values is presented in Figure 10. The figure shows good agreement. Thus, the earlier conclusion of goodness-of-fit can be justified.

The unsuitability of the model, developed for inner surface contact angle, is most likely due to the relatively small change in the contact angle data, i.e., from 81.5° to 89.1°, with only few exceptions of M7

TABLE XI
Analysis of Variance (ANOVA) Table for Model; Response: Membrane Porosity of SMM-Modified Membranes

Source	DF[a]	Seq SS[b]	Adj SS	Adj MS[c]	F	F-tabulated	P
Regression	4	3.46E-03	3.46E-03	8.64E-04	6.63	3.0556	0.003
Residual error	15	1.95E-03	1.95E-03	1.30E-04			
Lack-of-fit	10	1.32E-03	1.32E-03	1.32E-04	1.04	4.7351	0.514
Pure error	5	6.34E-04	6.34E-04	1.27E-04			
Total	19	5.41E-03					

$R^2 = 63.88\%$; $R^2_{\text{adjusted}} = 54.25\%$.
[a] DF, degree of freedom.
[b] SS, sum of squares.
[c] MS, mean square.

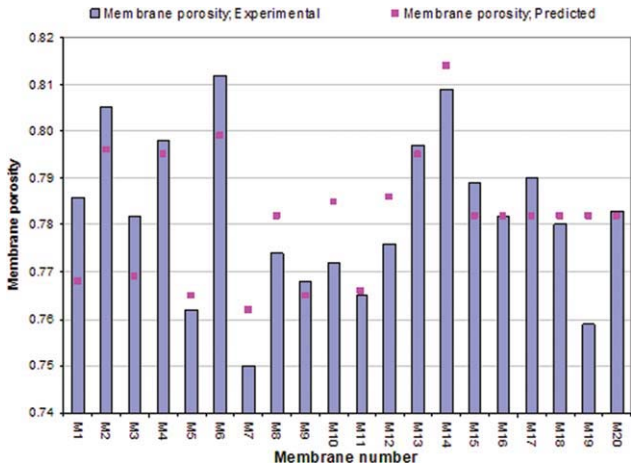

Figure 7 Comparison of experimental results and predicted values by model for membrane porosity for membranes with SMM. [Color figure can be viewed in the online issue, which is available at wileyonlinelibrary.com.]

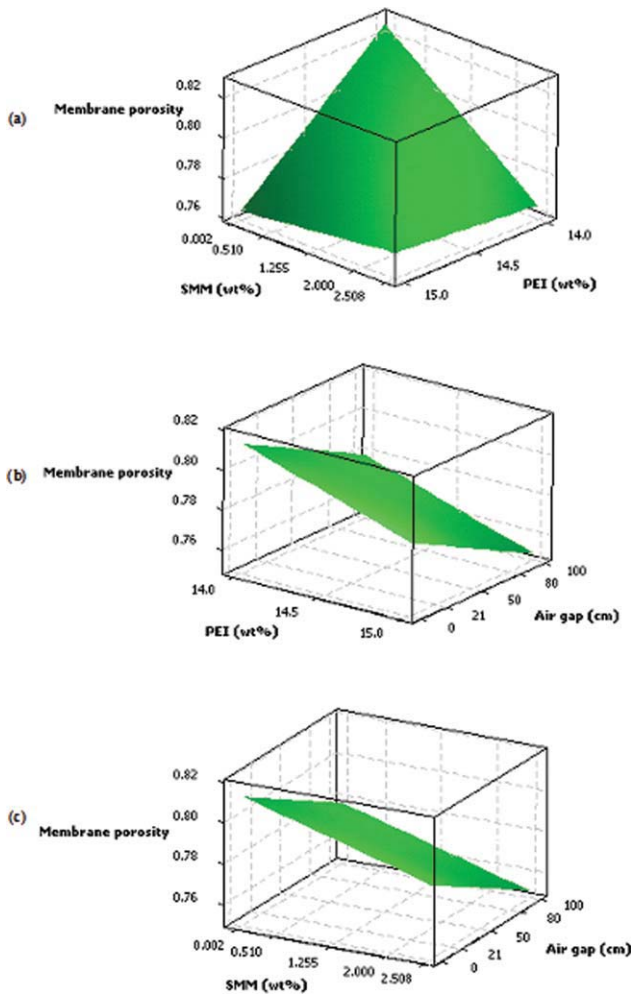

Figure 8 The surface plots for membrane porosity, (a) PEI (wt %) and SMM (wt %), air gap value: 50.5 cm; (b) PEI (wt %) and air gap (cm), SMM (wt %) value: 1.255; and (c) SMM (wt %) and air gap (cm), PEI (wt %) value: 14.5. [Color figure can be viewed in the online issue, which is available at wileyonlinelibrary.com.]

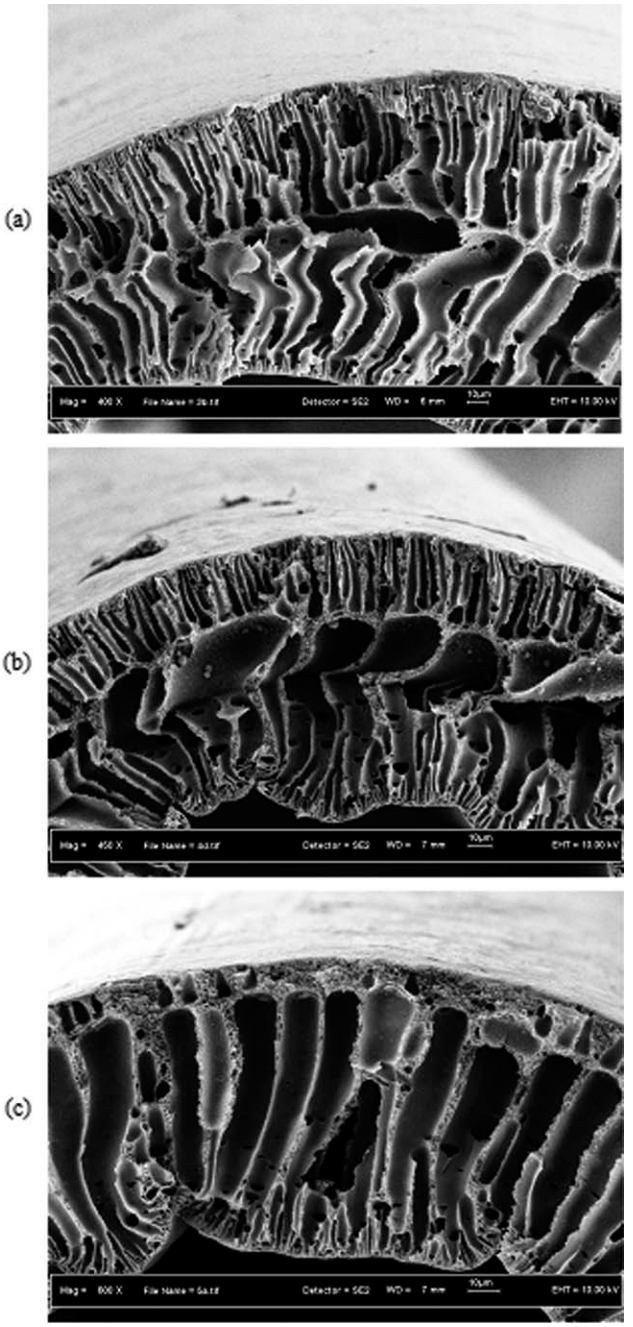

Figure 9 SEM micrographs of membranes cross section, (a): No. M6, (b): No. M16, and (c): No. M5.

(76.8°), M10 (72.3°), and M15 (92.1°). The scatter of the data from the hollow fibers M15 to M20 (82.0°–92.1°) is also very large even though the hollow fibers were fabricated under the same conditions. Moreover, the contact angle depends not only on hydrophobicity but also on other surface properties such as pore size and surface roughness.

The nearly constant value of the inner surface contact angle was also reported elsewhere.[24] The inner surface contact angle of SMM-modified PES membranes changed from 37° and 53° with an increase in air gap, and this change is considered insignificant.

TABLE XII
Estimated Regression Coefficients (Coded Factors), Response: Inner Surface Contact Angle

Term	Coefficient	S.E. coefficient	t	P
Constant	85.4428	1.201	71.132	0.000
x_1: PEI (wt %)	−2.4887	1.912	−1.302	0.214
x_2: SMM (wt %)	0.9753	1.912	0.510	0.618
x_3: Air gap (cm)	0.8284	1.912	0.433	0.671
x_1^2: PEI (wt %) × PEI (wt %)	−4.8579	3.101	−1.566	0.140
$x_2\ x_3$: SMM (wt %) × Air gap (cm)	−7.0355	4.200	−1.675	0.116

It is worth noting that the average value of the inner surface contact angle was 84.3° which was higher than that of hollow fibers without SMM (80.6°). This is due to the presence of SMM in the membrane, even though SMM surface migration hardly took place, because of the instant solidification of polymer, after the dope extrusion from the spinneret.

ANOVA for outer surface contact angle

The response surface methodology in Minitab software, release 15 was used to find the best model for the outer surface contact angle. The estimated coefficients for the model in terms of coded factors and the P-value and t-value for each coefficient are shown in Table XIV.

Considering the P-values and t-values of coefficients, the significant terms in the model for the outer surface contact angle can be ranked as follows:

$$x_3^2 > x_2 > x_1 > x_3$$

The ANOVA at 95% confidence limit for the model developed for the outer surface contact angle is shown in Table XV.

The F-value for the model is 5.41 which is greater than the tabulated F-value at 95% confidence limit, $F_{0.05}(f_1,f_2) = F_{0.05}(4,15) = 3.0556$. The F-value for the lack-of-fit, which is 18.18, is not lower than the tabulated F-value, $F_{0.05}(f_3,f_4) = F_{0.05}(10,5) = 4.7351$. Also, the P-value for the model is 0.007, which is smaller than 0.05. The P-value for the lack-of-fit is 0.003, which is not greater than 0.05. Therefore, although the model satisfies the criteria for regression validity, its goodness-of-fit is not suitable. Moreover, R^2 and R^2-adjusted for the model are 59.04% and 48.12%, respectively, which are small for R^2.

The low accuracy of the model can be related to the effect of other surface properties on contact angle. It was reported that changing the surface roughness can increase the hydrophobicity of surface.[42–44] Also, it was reported that contact angle of the hollow fiber membrane decreases with the increasing air gap.[24,45] These facts can be related to the effect of surface properties of membrane such as surface roughness, pore size, and surface porosity on contact angle.

Since the contact angle of the membrane surface depends both on the hydrophobicity of polymer and also on the properties of the surface, the accuracy of the developed model is low. It is known that the fabrication parameters can affect the surface properties such as surface roughness, pore size, and surface porosity, and these properties can in turn affect the contact angle. Therefore, the contact angle is a complicated function of fabrication parameters and the developed model can not represent such a complicated function.

Comparison of the experimental and predicted values for the outer surface contact angle is presented in Figure 11, which shows that fitting of the model is rather poor.

Effect of membrane fabrication parameters on outer surface contact angle

The surface plots of the outer surface contact angle versus two fabrication parameters, whereas the third fabrication parameter is set at its central value, are shown in Figure 12(a–c).

TABLE XIII
Analysis of Variance (ANOVA) Table for Model; Response: Inner Surface Contact Angle of SMM-Modified Membranes

Source	DF[a]	Seq SS[b]	Adj SS	Adj MS[c]	F	F-tabulated	P
Regression	5	130.60	130.60	26.12	1.48	2.9582	0.258
Residual error	14	247.02	247.02	17.64			
Lack-of-fit	9	172.63	172.63	19.18	1.29	4.7725	0.409
pure error	5	74.39	74.39	14.88			
Total	19	377.62					

$R^2 = 34.58\%$; $R^2_{\text{adjusted}} = 11.22\%$.
[a] DF, degree of freedom.
[b] SS, sum of squares.
[c] MS, mean square.

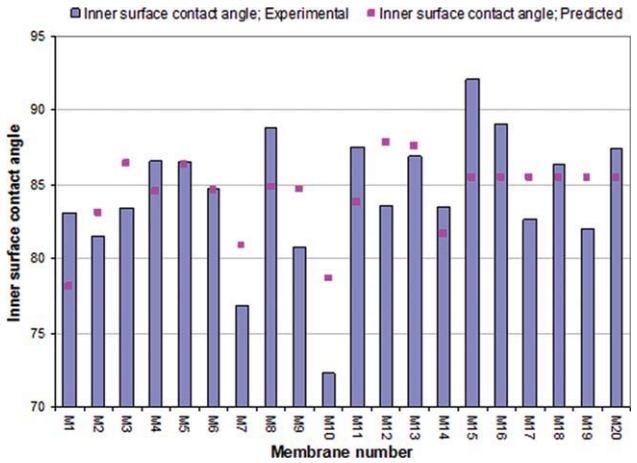

Figure 10 Comparison of experimental results and predicted values by model for inner surface contact angle for membranes with SMM. [Color figure can be viewed in the online issue, which is available at wileyonlinelibrary.com.]

Figure 12(a) shows that, for a given PEI concentration, the contact angle increases linearly with SMM concentration. This is natural considering the hydrophobic nature of SMM. Figure 12(a) also shows that, for a given SMM concentration, the contact angle increases linearly with an increase in the PEI concentration. This is probably due to the decrease in surface pore size and porosity of the PEI hollow fiber as PEI concentration increases.

Figure 12(b,c) demonstrate that for given values of PEI and SMM concentrations, a maximum appears in the contact angle as the air gap increases. This seems to be a result of super-imposition of two opposing effects of air-gap on the SMM surface migration. One: as the nascent hollow fiber travels along the air gap for a longer period, more SMM migrates to the outer surface of the hollow fiber, which increases hydrophobicity and contact angle. The other: due to elongation of the hollow fiber, polymer molecules are oriented to axial direction, decreasing the entropy. The decrease in entropy is compensated by an increase in enthalpy, which leads to redistribution of SMM at the outer surface. As a result, the SMM concentration at the surface is reduced. This view is justified by the EDX data summarized in Table XVI. As the air gap increases, the atomic concentration of both Si and F, the markers of the SMM, shows a maximum. This coincides with the maximum observed in contact angle.

Also the effect of other surface properties such as pore size should be considered. As was shown in "Effect of membrane fabrication parameters on mean pore size ($r_{P,m}$)", the plot of $r_{P,m}$ versus air gap shows a minimum value. As the pore size on the surface of membrane can affect the contact angle, the effect of $r_{P,m}$ trend versus air gap on the contact angle should be considered.

TABLE XIV
Estimated Regression Coefficients (Coded Factors), Response: Outer Surface Contact Angle

Term	Coefficient	S.E. coefficient	t	P
Constant	94.646	1.107	85.478	0.000
x_1: PEI (wt %)	2.794	1.762	1.585	0.134
x_2: SMM (wt %)	3.673	1.762	2.084	0.055
x_3: Air gap (cm)	2.765	1.762	1.569	0.137
x_3^2: Air gap (cm) × Air gap (cm)	−10.027	2.859	−3.507	0.003

CONCLUSIONS

Response Surface Methodology (RSM) was used to find the effect of Surface Modifying Macromolecule (SMM) on the properties of polyetherimide (PEI) hollow fiber membranes. Three fabrication parameters, which are PEI and SMM concentrations in casting dope and air gap, were selected as variables, while the characterization tests results, which are the mean pore size ($r_{P,m}$), gas permeation rate, membrane porosity, and contact angle of water at the inner and outer surface of the membranes, were

TABLE XV
Analysis of Variance (ANOVA) Table for Model; Response: Outer Surface Contact Angle of SMM-Modified Membranes

Source	DF[a]	Seq SS[b]	Adj SS	Adj MS[c]	F	F-tabulated	P
Regression	4	324.151	324.151	81.038	5.41	3.0556	0.007
Residual error	15	224.887	224.887	14.992			
Lack-of-fit	10	218.852	218.852	21.885	18.13	4.7351	0.003
pure error	5	6.035	6.035	1.207			
Total	19	549.038					

$R^2 = 59.04\%$; $R^2_{\text{adjusted}} = 48.12\%$.
[a] DF, degree of freedom.
[b] SS, sum of squares.
[c] MS, mean square.

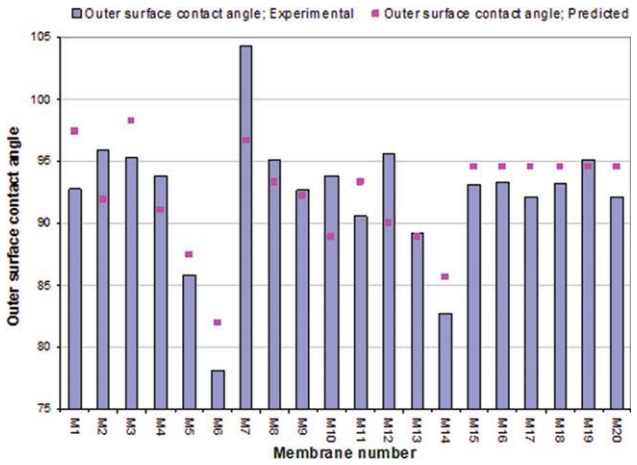

Figure 11 Comparison of experimental results and predicted values by model for outer surface contact angle for membranes with SMM. [Color figure can be viewed in the online issue, which is available at wileyonlinelibrary.com.]

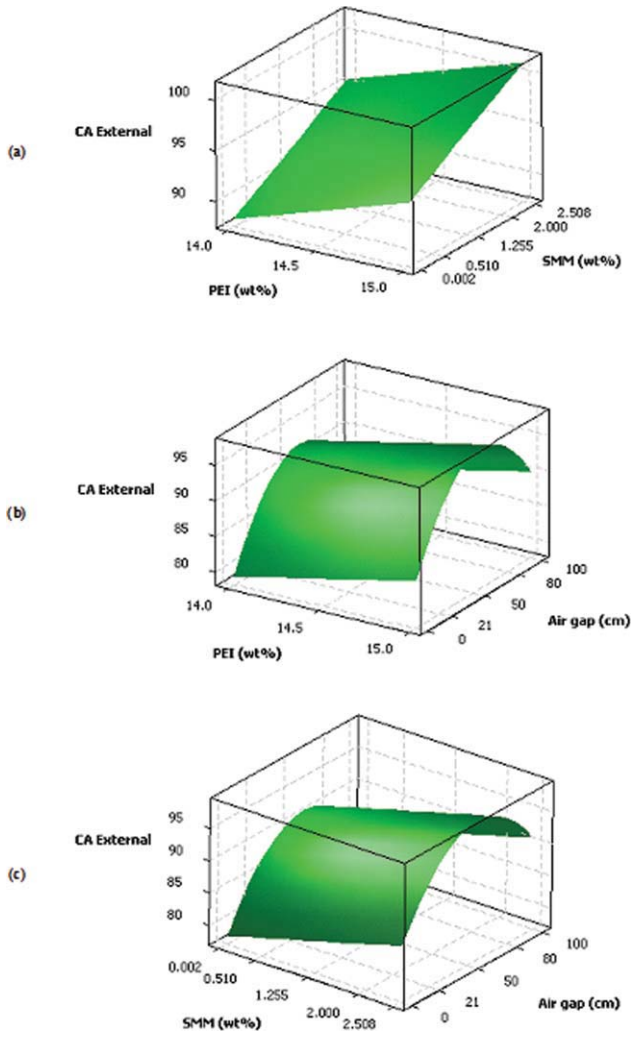

Figure 12 The surface plots for outer surface contact angle, (a) PEI (wt %) and SMM (wt %), air gap value: 50.5 cm; (b) PEI (wt %) and air gap (cm), SMM (wt %) value: 1.255; and (c) SMM (wt %) and air gap (cm), PEI (wt %) value: 14.5. [Color figure can be viewed in the online issue, which is available at wileyonlinelibrary.com.]

TABLE XVI
EDX Test Results for F (wt %) and Si (wt %) on the Outer Surface of Membranes No. M6, No. M16, and No. M5

Membrane number	PEI (wt %)	SMM (wt %)	Air gap (cm)	F (wt %)	Si (wt %)
M6	14.50	1.255	0.89	0.37	3.19
M16	14.50	1.255	50.50	0.83	7.74
M5	14.50	1.255	100.11	0.20	1.30

selected as responses. The conclusions are as follows:

1. Compared with the PEI membranes without SMM, the SMM-modified membranes have generally higher mean pore size, permeation rate, inner and outer surface contact angle but lower membrane porosity.
2. The regression model developed for mean pore size, $r_{P,m}$, satisfies all the statistical criteria. The plot of $r_{P,m}$ versus air gap shows a minimum value for $r_{P,m}$, which value depends on the PEI and SMM concentrations in the spinning dope. This is because of the effects of the absorption of water vapor into the nascent fiber, coalescence of polymer aggregates on the outer surface of the fiber and fiber elongation. The plots of $r_{P,m}$ versus PEI and SMM concentrations in the spinning dope show a maximum. This is because of the various effects of SMM on the PEI solution such as increasing the solid content and viscosity, as well as promoting the phase inversion process.
3. The regression model obtained for gas permeation rate has good statistical parameters and can be used for prediction of permeation rate. The model does not offer any dependency of gas permeation rate on SMM concentration in the spinning dope. The model predicts a minimum value for permeation rate versus air gap and a maximum value versus the PEI concentration, which coincides the trend in $r_{P,m}$ versus air gap and the PEI concentration.
4. The regression model developed for membrane porosity satisfies the statistical criteria for F-value and P-value but it has relatively low R^2. The model predicts that membrane porosity decreases as air gap increases, which is related to coalescence on the outer surface of the fiber and formation of thicker skin layer due to the VIPS process. In addition, the model predicts that the trend of membrane porosity versus PEI concentration depends on SMM concentration, which means that there is an interaction between the effects of PEI concentration and SMM concentration on the membrane porosity.

5. The model developed for inner surface contact angle has low accuracy and does not satisfy any of the statistical criteria. This is because of the effect of the bore fluid on the inner surface of membranes since water was used as the bore fluid. The model developed for the outer surface contact angle has low R^2 and predicts that the contact angle increases with an increase in the SMM concentration in the spinning dope and shows a maximum when the air gap is changed. This can be explained by the opposite effects of SMM migration to the outer surface and elongation of the nascent fiber, which contributes to the redistribution of SMM at outer surface. It is interesting to note that the same trend was observed for SMM concentration on the outer surface of membrane.

NOMENCLATURE

A_P	area of pores (m^2)
A_T	total area of membrane (m^2)
$\{a_i\}$	coefficients of the regression model
$\{a_{ii}\}$	coefficients of the regression model
$\{a_{ij}\}$	coefficients of the regression model
E	overall shrinkage of membrane during drying
f	number of factors
f_1	degree of freedom for regression
f_2	degree of freedom for residual error
f_3	degree of freedom for lack-of-fit
f_4	degree of freedom for pure error
G	mass fraction of polymer in the membrane
L_P	effective pore length (m)
M	molecular weight of Helium gas (Kg mol^{-1})
M_n	number average molecular weight
m	number of the urea repeating unit in SMM
n	number of the PDMS repeating unit in SMM
PDI	polydispersity index
p	number of the CF_2 repeating unit in SMM
p_u	upstream pressure (Pa)
p_d	downstream pressure (Pa)
R	universal gas constant (8.314 J mol^{-1} K^{-1})
R^2	coefficient of regression
$r_{P,m}$	mean pore radius (m)
S_l	the longitudinal shrinkage of hollow fiber
T	absolute temperature (K)
$\{x_i\}$	linear terms in the regression model
$\{x_i^2\}$	quadratic terms in the regression model
$\{x_i x_j\}$	interaction terms in the regression model
Y	response (experimental data)
α	axial spacing
ε	membrane porosity
ρ_P	polymer density (g cm^{-3})
ρ_m	membrane density (g cm^{-3})
ρ_{water}	density of water (g cm^{-3})
μ	viscosity of gas (Pa.s)
ξ	surface porosity
ζ	error between experimental data and the results predicted by model

References

1. Khayet, M.; Abu Seman, M. N.; Hilal, N. J Membr Sci 2010, 349, 113.
2. Khayet, M.; Chowdhury, G.; Matsuura, T. AIChE J 2002, 48, 2833.
3. Zhang, L.; Chowdhury, G.; Feng, C.; Matsuura, T.; Narbaitz, R. J Appl Polym Sci 2003, 88, 3132.
4. Qiu, C.; Nguyen, Q. T.; Ping, Z. J Membr Sci 2007, 295, 88.
5. Yusof, A. H. M.; Ulbricht, M. J Membr Sci 2008, 311, 294.
6. Hilal, N.; Al-Khatib, L.; Atkin, B. P.; Kochkodan, V.; Potapchenko, N. Desalination 2003, 158, 65.
7. Taniguchi, M.; Belfort, G. J Membr Sci 2004, 231, 147.
8. Kilduff, J. E.; Mattaraj, S.; Pieracci, J. P.; Belfort, G. Desalination 2000, 132, 133.
9. Chennamsetty, R.; Escobar, I. Langmuir 2008, 24, 5569.
10. Turan, E.; Caykara, T. J Appl Polym Sci 2007, 106, 2000.
11. Freger, V.; Gilron, J.; Belfer, S. J Membr Sci 2002, 209, 283.
12. Chen, H.; Belfort, G. J Appl Polym Sci 1999, 72, 1699.
13. Ulbricht, M.; Belfort, G. J Membr Sci 1996, 111, 193.
14. Pham, V. A.; Santerre, J. P.; Matsuura, T.; Narbaitz, R. M. J Appl Polym Sci 1999, 73, 1363.
15. Bolong, N.; Ismail, A. F.; Salim, M. R.; Rana, D.; Matsuura, T. J Membr Sci 2009, 331, 40.
16. Suk, D. E.; Pleizier, G.; Deslandes, Y.; Matsuura, T. Desalination 2002, 149, 303.
17. Khayet, M.; Suk, D. E.; Narbaitz, R. M.; Santerre, J. P.; Matsuura, T. J Appl Polym Sci 2003, 89, 2902.
18. Suk, D. E.; Chowdhury, G.; Matsuura, T.; Narbaitz, R. M.; Santerre, P.; Pleizier, G.; Deslandes, Y. Macromolecules 2002, 35, 3017.
19. Hamza, A.; Pham, V. A.; Matsuura, T.; Santerre, J. P. J Membr Sci 1997, 131, 217.
20. Rana, D.; Matsuura, T.; Narbaitz, R. M.; Feng, C. J Membr Sci 2005, 249, 103.
21. Khayet, M.; Feng, C. Y.; Matsuura, T. J Membr Sci 2003, 213, 159.
22. Khayet, M. Appl Surf Sci 2004, 238, 269.
23. Mosqueda-Jimenez, D. B.; Narbaitz, R. M.; Matsuura, T. Sep Purif Technol 2004, 37, 51.
24. Khulbe, K. C.; Feng, C. Y.; Matsuura, T.; Mosqueada-Jimenaez, D. C.; Rafat, M.; Kingston, D.; Narbaitz, R. M.; Khayet, M. J Appl Polym Sci 2007, 104, 710.
25. Wang, K. Y.; Matsuura, T.; Chung, T. S.; Guo, W. F. J Membr Sci 2004, 240, 67.
26. Khayet, M.; Garcia-Payo, M. C.; Qusay, F. A.; Khulbe, K. C.; Feng, C. Y.; Matsuura, T. J Membr Sci 2008, 311, 259.
27. Qian, H.; Zhang, Y. X.; Huang, S. M.; Lin, Z. Y. Appl Surf Sci 2007, 253, 4659.
28. Nguyen, A. H.; Narbaitz, R. M.; Matsuura, T. J Environ Eng 2007, 133, 515.
29. Tasselli, F.; Jansen, J. C.; Sidari, F.; Drioli, E. J Membr Sci 2005, 255, 13.
30. Mosqueda-Jimenez, D. B.; Narbaitz, R. M.; Matsuura, T.; Chowdhury, G.; Pleizier, G.; Santerre, J. P. J Membr Sci 2004, 231, 209.
31. Xiarchos, I.; Jaworska, A.; Zakrzewska-Trznadel, G. J Membr Sci 2008, 321, 222.
32. Qtaishat, M.; Rana, D.; Matsuura, T.; Khayet, M. AIChE J 2009, 55, 3145

33. Ismail, A. F.; Dunkin, I. R.; Gallivan, S. L.; Shilton, S. J. Polymer 1999, 40, 6499.
34. Li, K. Ceramic Membranes for Separation and Reaction, John Wiley & Sons, Chichester, England, 2007.
35. Khayet, M.; Feng, C. Y.; Khulbe, K. C.; Matsuura, T. Desalination 2002, 148, 321.
36. Fontananova, E.; Jansen, J. C.; Cristiano, A.; Curcio, E.; Drioli, E. Desalination 2006, 192, 190.
37. Ismail, A. F.; Kumari, S. N. J Membr Sci 2004, 236, 183.
38. Chabot, S.; Roy, C.; Chowdhury, G.; Matsuura, T. J Appl Polym Sci 1997, 65, 1263.
39. Myers, R. H.; Montgomery, D. C. Response Surface Methodology: Process and Product Optimization Using Designed Experiments; Wiley: New York, 2002.
40. Khayet, M. Chem Eng Sci 2003, 58, 3091.
41. Wang, D.; Li, K.; Teo, W. K. J Membr Sci 1998, 138, 193.
42. Wang, K. Y.; Chung, T. S.; Gryta, M. Chem Eng Sci 2008, 63, 2587.
43. Zhao, N.; Xie, Q.; Weng, L.; Wang, S.; Zhang, X.; Xu, J. Macromolecules 2005, 38, 8996.
44. Peng, M.; Li, H.; Wu, L.; Zheng, Q.; Chen, Y.; Gu, W. J Appl Polym Sci 2005, 98, 1358.
45. Khulbe, K. C.; Feng, C.; Matsuura, T.; Kapantaidakis, G. C.; Wessling, M.; Koops, G. H. J Membr Sci 2003, 226, 63.